Dipole Alignment at the Carbon Nanotube and Methyl Ammonium Lead Iodide Perovskite Interface

Joshua Przepioski

SLAC National Accelerator Laboratory, 2575 Sand Hill Rd, 94025, Menlo Park CA, USA

This work correlates resonant peaks from first principles calculation on ammonia (NH_3) Nitrogen 1s x-ray absorption spectroscopy (XAS) within the methyl ammonium lead iodide perovskite ($CH_3NH_3PbI_3$), and proposes a curve to determine the alignment of the methyl ammonium dipole if there exists angular dependence. The Nitrogen 1s XAS was performed at varying incident angles on the perovskite with and without a carbon nanotube (CNT) interface produced from an ultrasonic spray deposition. We investigated the peak contribution from PbI_2 and the poly(9,9-dioctylfluorene-2,7-diyl) with bipyridine (PFO-BPy) wrapped around the CNT, and used normalization techniques to better identify the dipole alignment. There was angular dependence on samples containing the CNT interface suggesting an existing dipole alignment, but there was no angular dependence on the perovskite samples alone; however, more normalization techniques and experimental work must be performed in order to ensure its validity and to better describe its alignment, and possible controlling factors.

INTRODUCTION

Solar cells have gained the attention of many researchers with hopes of mitigating future carbon emission from energy sources, which has been proven to have a relationship with global warming. The most typical solar cells are made by doped layers of silicon or a combination of elements from the III-V table and buffer layers, and with nearly 40 years of research shown by NREL's Best Research-Cell Efficiencies chart, these cells are reaching a power conversion efficiency (PCE) of 46%; however, negligible improvement rates in their cost and performance has led researchers, as well as the industry, to seek cheaper and Earth abundant alternatives. Among these alternatives, the perovskite family has been considered for solar cells within a mere 5 ~ 6 years, and it has already achieved a PCE greater than 20%. [1] The performance of the solar cells is critically dependent on the efficiency of charge transfer across the interfaces in a real device, and many of these properties for the perovskite family are not well understood. We will study this aspect for a model interface of CNT on a perovskite, which has shown premise.[2] In particular, the alignment of methyl ammonium dipole inside of the methyl ammonium trihalide perovsikites can modify the electronic levels near the interface.[3] The role of the methyl ammonium dipole inside of the perovskite has been inferred in previous papers, but it has not been confirmed.[4,5] We will use first principles calculation to describe the dipole's alignment and perform XAS to confirm the alignment experimentally, which may give insight about its

This material is based upon work supported by the U.S. Department of Energy, Office of Science, Office of Workforce Development for Teachers and Scientists (WDTS) under the Science Undergraduate Laboratory Internship (SULI) program, under Contract No. DE-AC02-76SF00515.

mechanism in the electron mobility, charge transport, electronic structure, and possible leads to further improve their efficiency.

EXPERIMENTAL WORK

First principles calculations using StoBe were used to optimize the geometry of ammonia (NH_3) and for angular dependent x-ray spectra with a planar electric field.[6] The nitrogen atom was fixed to the origin with the hydrogen atoms sitting below the xy-plane, and it was optimized into $C_{3,v}$ symmetry, which has shown to give valid generalizations.[7] The x-ray spectra calculations were performed by varying the incident angle. We plotted the $4a_1$* and 2e* amplitude corresponding to each polar angle, θ, from 0º to 90º in increments of 10º, and we used a periodic curve to closely fit each point; we also confirmed that varying the azimuth angle, φ, had no effect because the electric field was planar. We propose using this curve for experimental XAS to describe the alignment.

$CH_3NH_3PbI_3$ perovskites were prepared by a solvent mixture technique previously done by Jeon et. al[8] onto a glass, F-doped SnO_2 (FTO), and TiO_2 stack, with half the samples having a CNT layer from ultrasonic spray deposition.[9] The samples were left in an inert gas except for when the CNT layer sprayed onto the perovskite. The N 1s XAS was performed on each sample at Stanford Radiation Light Source beam lines 8-2 and 10-1 varying the incident angle from 20º to 90º, and they were also tested for beam damage to ensure there were no energy shifts in progressive scans. In addition to the perovskite samples, gold, CNT on Au, the PFO-BPy on Au, and PbI_2 on FTO and glass were tested for a control sample and for normalization. The counts were measured from the auger electrons, sample current, and florescence light, and the data was normalized by the incoming current; the auger electrons and sample current provided the most profound curves, which were used for the analysis. The data was further normalized by removing linear lines, and implementing the Thomas-Reiche-Kuhn sum rule wherever reasonable in order to remove the background noise.[7]

CONCLUSION

The geometry optimization placed the hydrogen atoms to be planar with each other, but not with the nitrogen atom, which was fixed to the origin. The coordinates are given in Table I. The first principles supported angular dependence on the x-ray spectra for ammonia, and the ionization potential was 409.7 eV, although it has been experimentally found to be 406.6

eV..[7] There were three prominent peaks at 405.9, 407.7, and 408.9 eV as seen in fig. 1, and each respectively correlated to $4a_1$*, 2e*, and a Rydberg peak. The $4a_1$* would completely deplete if the electric field was across the xy-plane. Conversely, its amplitude would be its largest when the electric field was across the z-axis. The $4a_1$* peak had a noticeable relationship to XAS transitions to the $2p_z$ orbital, and given the dipole selection rule, peaks would only be detect for transitions to p-type oribtals. The 2e* peak would never completely deplete but it would be at its minimum amplitude when the electric field was along or parallel to the z-axis, and at its maximum amplitude when the electric field was across the xy-plane; the Rydberg peak would closely follow the 2e* trend, but its results are reasonable compared to previously reported research.[7,10] The amplitudes of each peak were plotted against θ, and a periodic curve was fitted to its trend. Clearly, scaled and shifted curves $cos^2(\theta)$ and $sin^2(\theta)$ could very closely approximate the amplitude for $4a_1$* and 2e* in fig. 2. The two curves were also related to each other because if $4a_1$* increased, then the 2e* peak would decrease; the converse is also true. The maximum amplitude of $4a_1$* and the minimum amplitude of 2e* is the theoretical alignment of the x-ray along the dipole C–N bond.

Experimental N 1s XAS was done on the CNT on Au, and on the PFO-BPy on Au at beam line 10-1, and the results are shown in fig. 3. The PFO-BPy had a noticeable peak at 396.6 eV, and the CNTs had strong peaks from the pyridine at 396.5 eV and nitrogen doping at 398.9 eV.[11,12] Scan on the cleansed Au samples, known to have no peaks in N 1s XAS, showed no contamination at beam line 10-1; however, there was an unidentified peak around the 400 eV region while using beam line 8-2 (fig. 4), which is believed to be possible contamination from pyridine. The perovskites, alone, had peak amplitudes invariant to the incident angle of the x-ray (fig. 5). Our perovskites had no angular dependence, which was different from the results reported by McLeod et. al because their paper suggests the perovskites made by the one-step method is angular dependent.[3] This suggests that other factors have larger role in the dipole's alignment. The perovskites with the CNT layer had possible angular dependence (fig. 6); however, there was no noticeable change to the $4a_1$* peak. This could be because of the bond between C–N, and first principles will need to be performed on methyl ammonium. The XAS on the PbI_2 on FTO and glass suggest that the Pb (4d transitions) (fig. 7) and the pyridine in the CNT is dominating also over the $4a_1$* peak in, in fig. 8, although this could be from the contamination noticed on the Au. If the entire peak contribution is from Pb or pyridine, our interpretation of $4a_1$* will require other methods. Pyridine and graphene have previously been reported to have angular dependence as well,[11,13] and we have not been able to propose a normalization technique which would remove their angular dependence from the dipole's dependence should it exist. Larger energy range x-ray absorption may help with CNT layer to help with normalization, and removing curves from experimental angular x-ray spectra on the CNT layer and pyridine alone. Pyridine also has multiple peaks and the ration between the prominent peak and another might be another normalization technique.[14] The periodic curve along the $4a_1$* and 2e* amplitudes for each angle (scaled in

fig. 8) was not consistent with the theoretical calculations because the change in amplitude between 70º and 90º is not periodic. Although the relationship between $4a_1$* and 2e* was still preserved, this was not true for the concavity of their fitted curve. Unusual amplitude change suggests an error with the current normalization, so the alignment could not be characterize without further study, but the CNT or pyridine may have a controlling factor in the methyl ammonium's alignment, which is supportive of the controlled energy levels between the interfaces.

ACKNOWLEDGEMENTS

The authors acknowledge technical assistance and insightful discussions Dennis Nordlund, D. Sokaras, C. Schwartz, and T.C. Weng SLAC National Accelerator Laboratory, and P. Schultz, S. Christensen, and J. Berry at the National Renewable Energy Laboratory (NREL). This work was supported in part by the U.S. Department of Energy, Office of Science, Office of Workforce Development for Teachers and Scientists (WDTS) under the Science Undergraduate Laboratory Internship (SULI) program.

REFERENCES

1. H.J. Snaith, “Perovskites: The Emergence of a New Era for Low-Cost, High-Efficiency Solar Cells”, J. Phys. Chem. Lett 4, 3623 (2013).
2. M.S. Kumar, T.H. Kim, S.H. Lee, S.M. Song, J.W. Yang, K.S. Nahm and E.-K. Suh, “Influence of electric field type on the assembly of single walled carbon nanotubes”, Chem. Phys. Lett. 383, 235 (2004).
3. J.A. McLeod, Z. Wu, P. Shen, B. Sun and L. Liu, “Self-Alignment of the Methylammonium Cations in Thin-Film Organometal Pervoskites”, J. Phys. Chem. Lett 5, 2863 (2014).
4. L. Zuo, Z. Gu, T. Ye, W. Fu, G. Wu and H. Chen, “Enhanced Photovoltaic Performance of $CH_3NH_3PbI_3$ Pervoskite Solar Cells through Interfacial Engineering Using Self-Assembling Monolayer”, J. Am. Chem. Soc. 137, 2674 (2015).
5. J.M. Frost, K.T. Butler, F. Brivio, C.H. Hendon, M. van Schilfgaarde and A. Walsh, “Atomistic Origins of High-Performance in Hybrid Halide Perovskite Solar Cells”, Nano Lett. 14, 2584 (2014).
6. StoBe-deMon version 3.3 (2014), K. Hermann and L.G.M. Pettersson, M.E. Casida, C. Daul, A. Goursot, A. Koester, E. Proynov, A. St-Amant, and D.R. Salahub. Contributing authors: V. Carravetta, H. Duarte, C. Friedrich, N. Godbout, M. Gruber, J. Guan, C. Jamorski, M. Leboeuf, M. Leetmaa, M. Nyberg, S. Patchkovskii, L. Pedocchi, F. Sim, L. Triguero, and A. Vela.
7. J. Stöhr, R. Gomer (editor), NEXAFS Spectroscopy (Springer, Berlin, 2003) pp. 12, 54, 72, 91, 276-290.
8. N.J. Jeon, J.H. Noh, Y.C. Kim, W.S. Yang, S. Ryu, and S. Seok, “Solvent Engineering for High-Performance Inorganic-Organic Hybrid Perovskites Solar Cells”, Nature Materials, 13(9), 897 (2014).
9. S.L. Guillot, K.S. Mistry, A.D. Avery, J. Richard, A.-M. Dowgiallo, P.F. Ndione, J. van de Lagemaat, M.O. Reese, and J.L. Blackburn, “Precision Printing and Optical Modeling of Ultrathin SWCNT/C_{60} Heterojunction Solar Cells”, Nanoscale, 7(15), 6556 (2015).
10. G.R. Wight and C.E. Brion, “K-Shell Excitation of CH_4, NH_3, H_2O, CH_3OH, CH_3OCH_3 and CH_3NH_3, by 2.5 keV Electron Impact”, J. Electron. Spectrosc., 4(1), pp. 25 (1974).
11. L. Zhao, R. He, K.T. Rim, T. Schiros, K.S. Kim, H. Zhou, C. Gutierrez, S.P. Chocklingam, C.J. Arguello, L. Palova, D. Nordlund, M.S. Hybertsen, D.R. Reichman, T.F. Heinz, P. Kim, A. Pinczuk, G.W. Flynn, and A.N. Pasupathy, "Visualizing Individual Nitrogen Dopants in Monolayer Graphene", Science, 333 (6045), pp. 999-1003 (2011).
12. Y.-H. Zhang, Y.-B. Chen, K.-G. Zhou, C.-H. Liu, J. Zeng, H.-L. Zang, and Y. Peng, "Improving Gas Sensing Properties of Graphene by Introducing Dopants and Defects: A First-Principles Study", Nanotechnology, 20(18), p. 185504 (2009).
13. J. Stohr, and D.A. Outka, “Determination of Molecular Orientations on Surfaces from the Angular Dependence of Near-Edge X-Ray-Absorption Fine-Structure Spectra”, Phys. Rev. B, 36(15), 7891 (1987).
14. C. Kolczewski, R. Puttner, O. Plashkevych, H. Agren, V. Staemmler, M. Martins, G. Snell, A.S. Schlachter, M. Sant'Anna, G. Kaindl, L.G.M. Pettersson, "Detailed study of pyridine at the C 1s and N 1s ionization thresholds: The influence of the vibrational fine structure." J. Chem. Phys, 115(14), 6426 (2001).

FIGURES

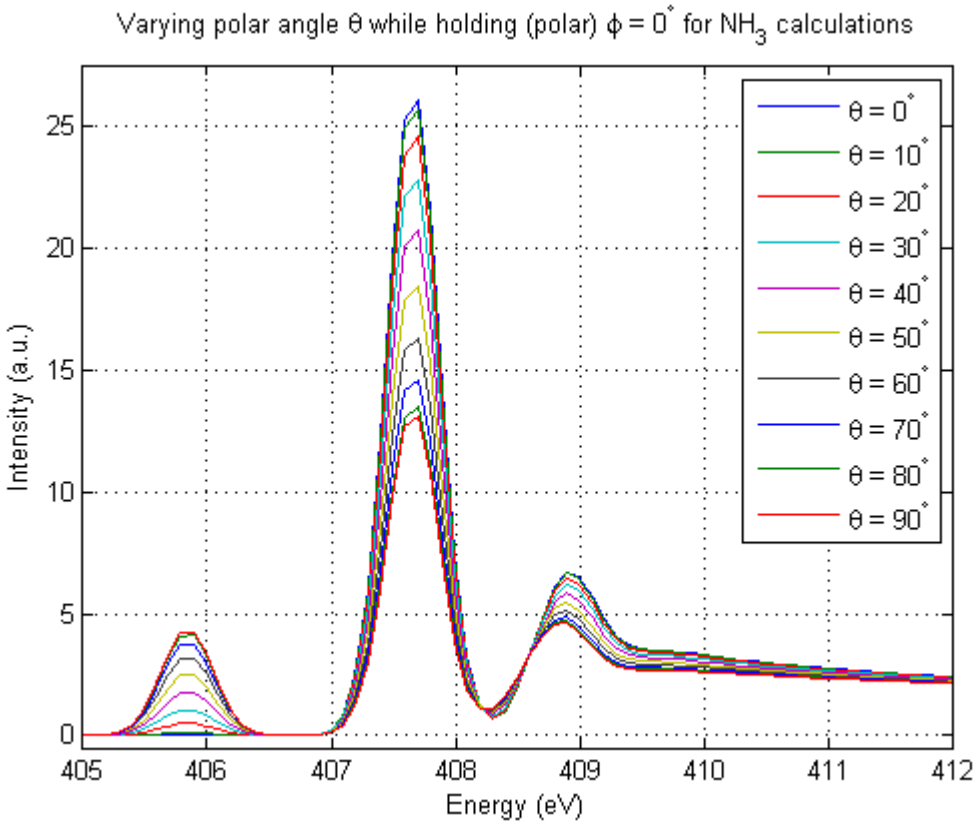

FIG. 1 Angular dependent x-ray spectra from first principles calculation on StoBe, and the three prominent peaks $4a_1$*, 2e*, and a Rydberg peak.

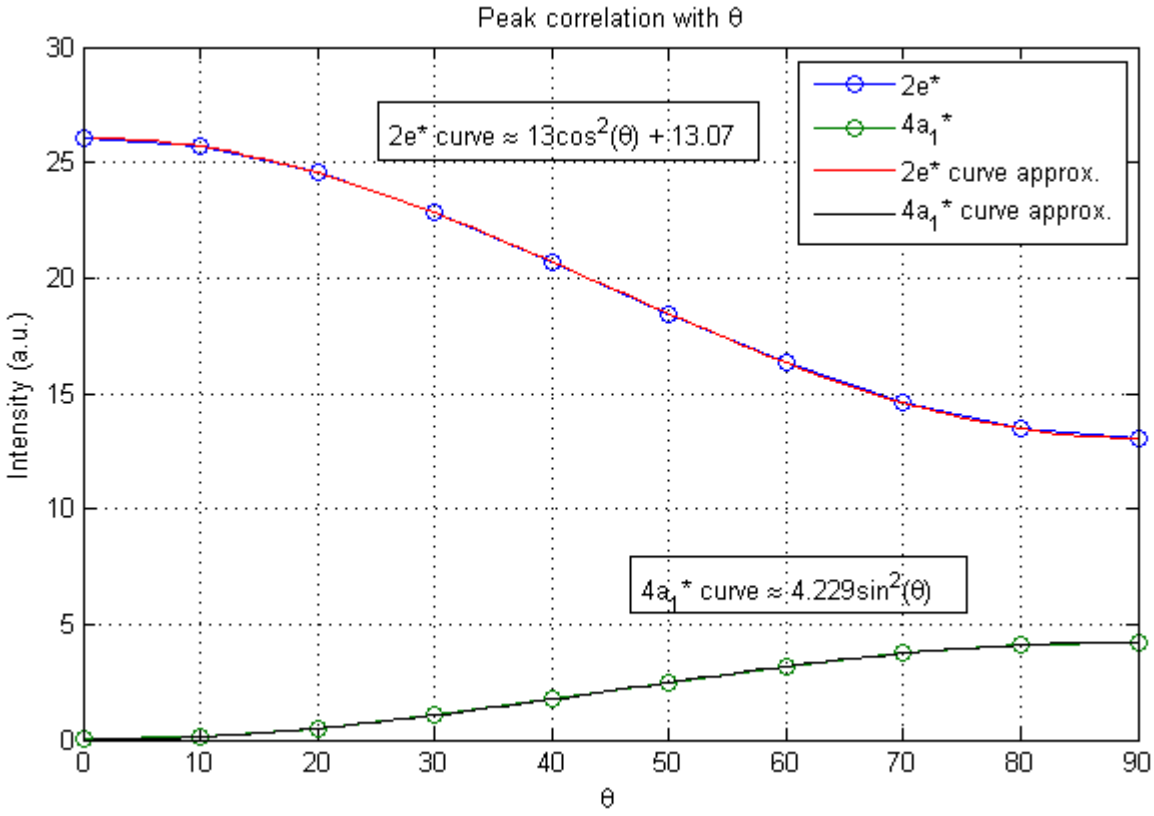

FIG. 2 Comparison of the $4a_1$* and 2e* peak from theoretical calculations, and proposed curves to fit XAS spectra.

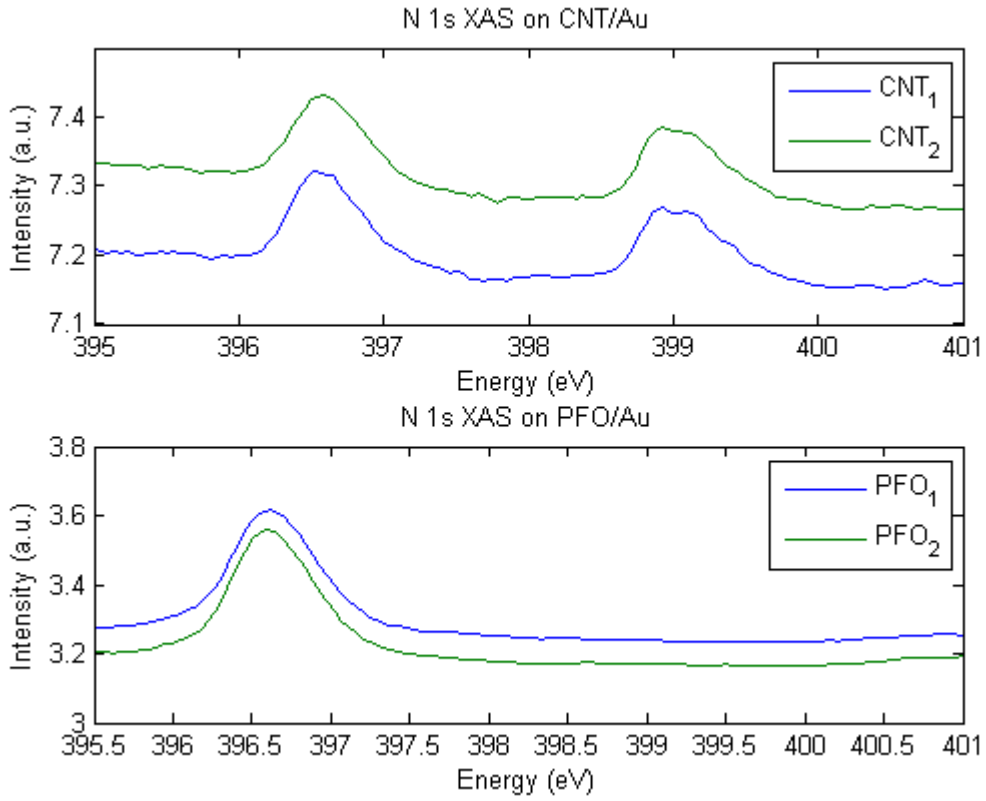

FIG. 3 Experimental N 1s XAS on CNT on Au, and on the PFO on Au.

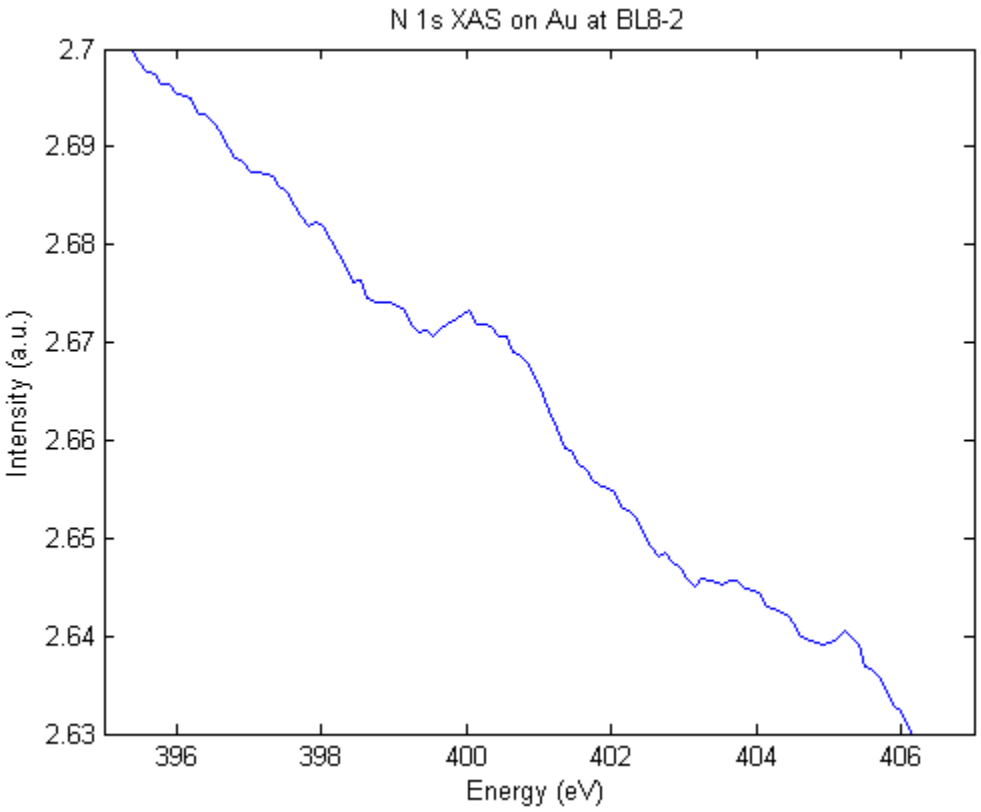

FIG. 4 Unknown peak from N 1s XAS on Au, which indicates possible contamination. Being near the 400 eV region we believe this contamination could be from the pyridine from other samples.

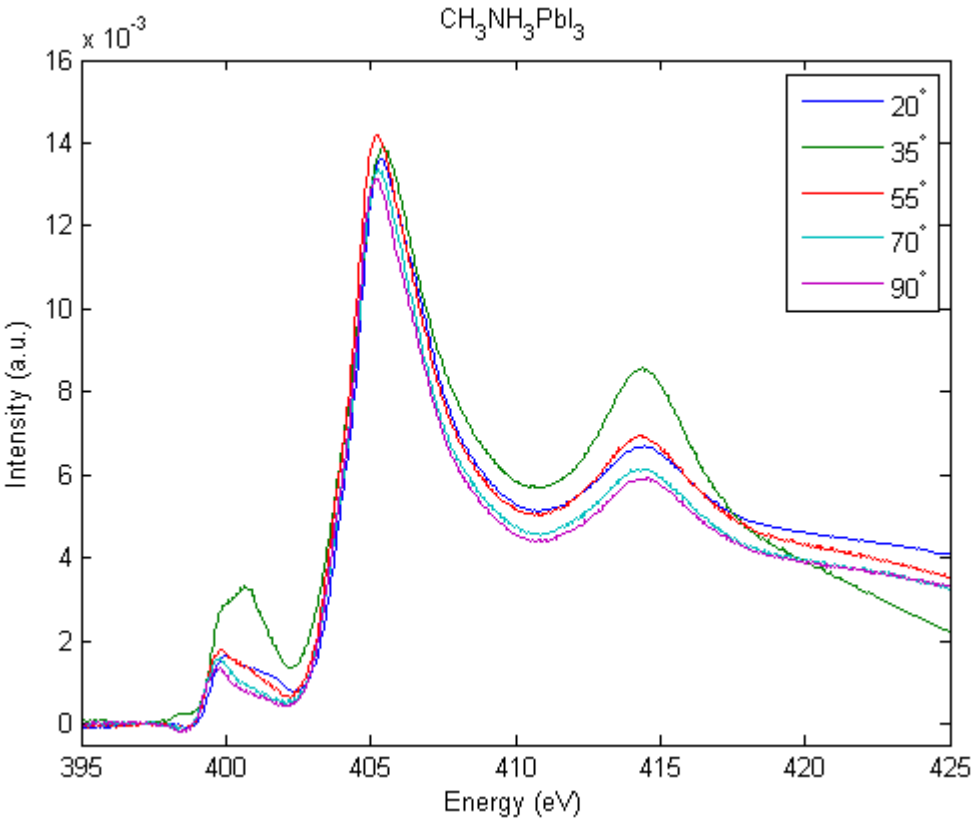

FIG. 5 The perovskite without CNT show no signs of angular dependence.

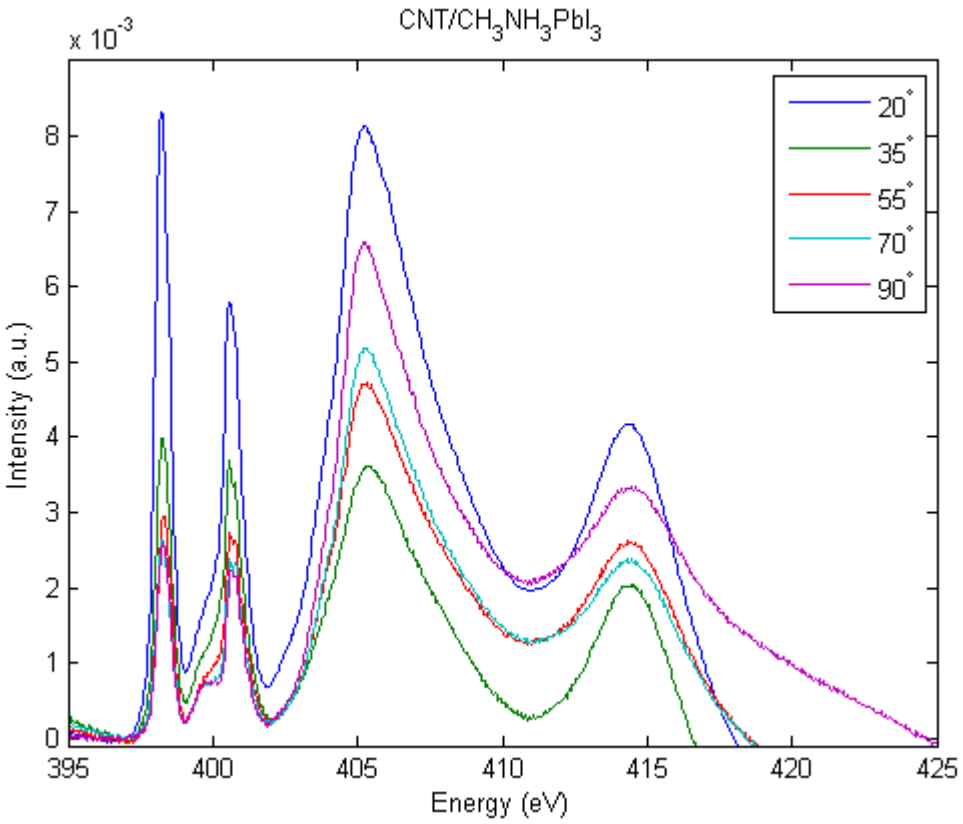

FIG. 6 Signs of angular dependence on the perovskite when the CNT layer is added. This data was partially normalized by removing a constant, but another line and scaling may reveal more about the peaks; also, the pyridine and CNTs alone are angular dependent.

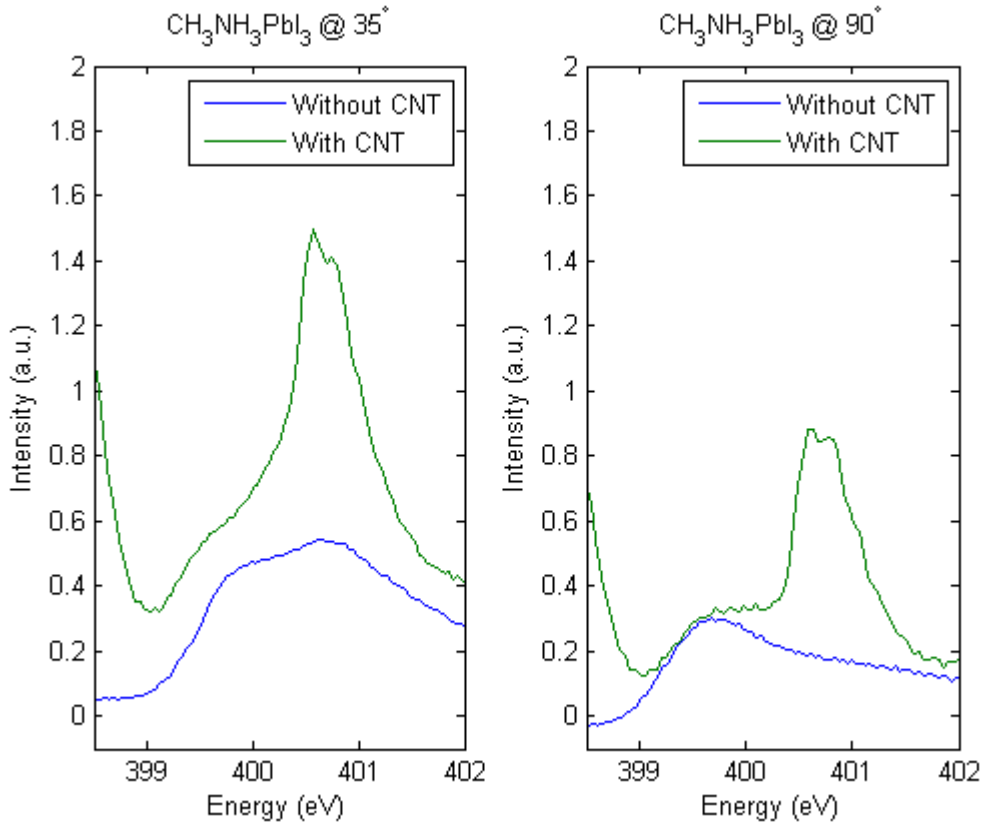

FIG. 7 The pyridine on the CNT produces a peak in XAS spectra that dominates over the $4a_1$* region. It is still possible to estimate the intensity of $4a_1$* because of a slight shift.

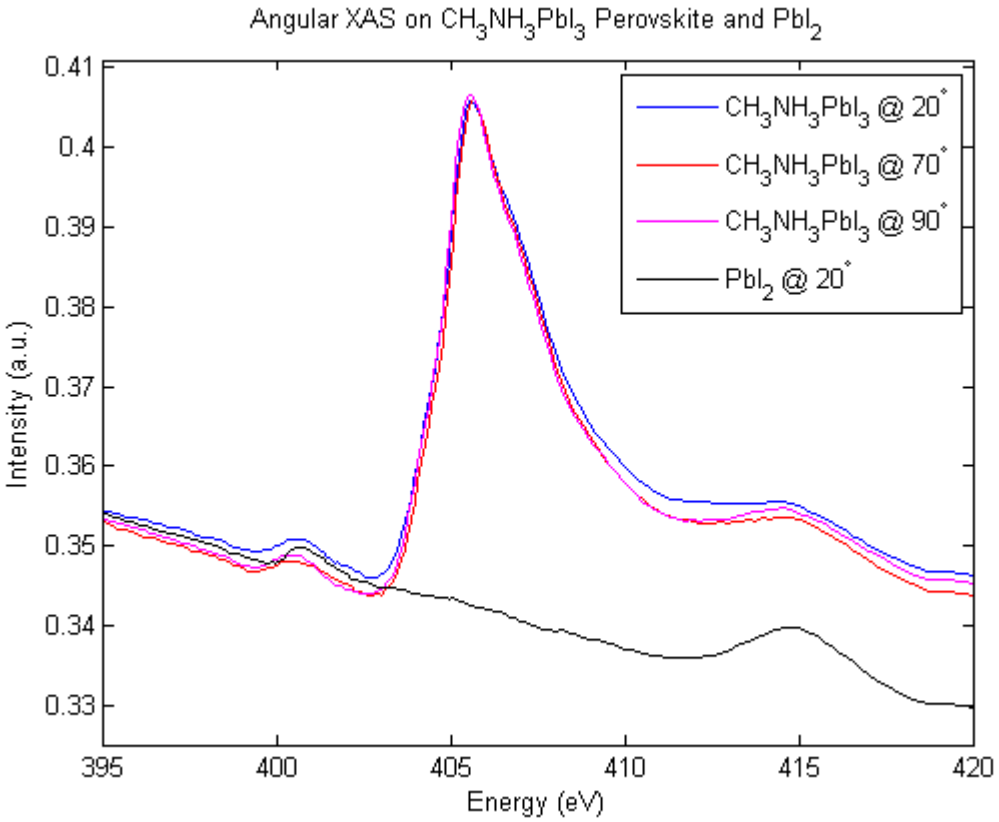

FIG. 8 The Pb curve dominates over $4a_1$* region and constructs onto the Rydberg region; however, further study needs to be done with the Pb. We are not sure if there is a shift in the Pb 4d orbitals inside of the perovskite although there should be no oxidation, but Pb directly above the $4a_1$* region was unexpected, and it could also be from the contamination noticed on Au.

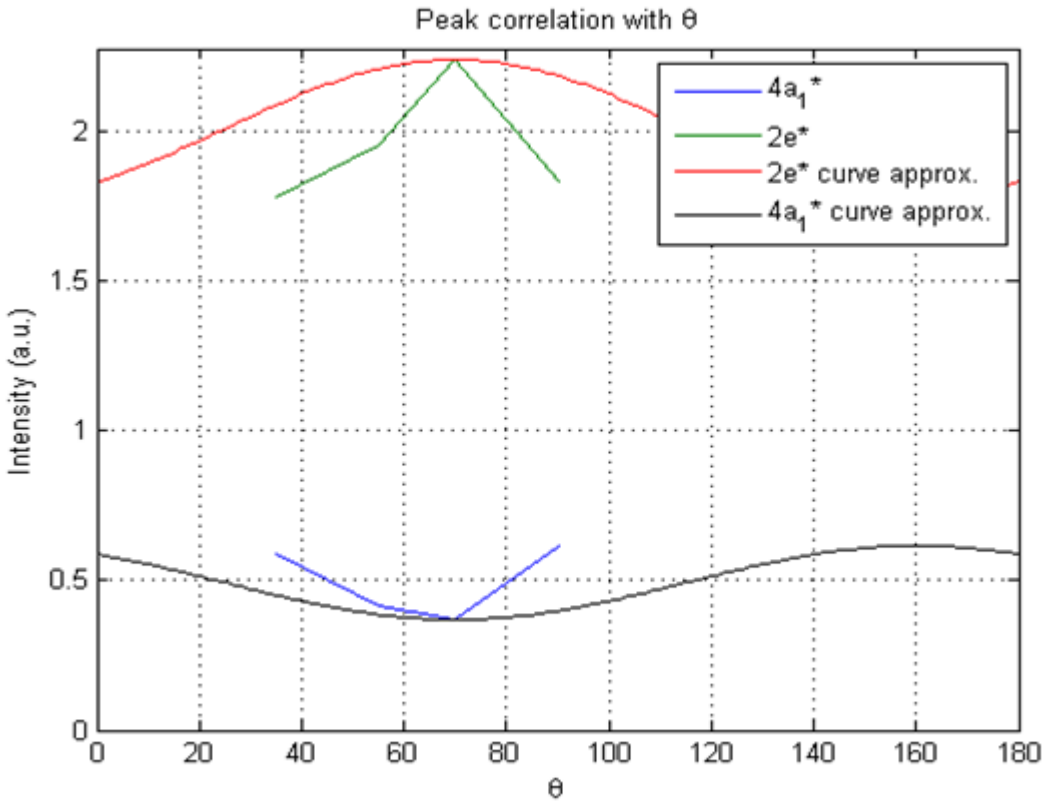

FIG. 9 The fitted curve on experimental amplitudes of $4a_1$* and 2e* from CNT/Perovskite interface, which were scaled, against the incident angle of the x-ray spectra. There is an unexpected change from 70° to 90°, which is not periodic.

TABLES

TABLE II. Optimized Cartesian coordinate in Angstroms for each atom in ammonia with $C_{3,v}$ symmetry used for the first principles calculation.

Atom	X	Y	Z
N	0.00000000	0.00000000	0.00000000
H	0.93505594	0.00000000	-0.41757551
H	-0.46752797	0.80978220	-0.41757551
H	-0.46752797	-0.80978220	-0.41757551